

Jiao Zhou

Key Laboratory of Dynamics and Control of
Flight Vehicle,
Ministry of Education,
School of Aerospace Engineering,
Beijing Institute of Technology,
Beijing 100081, China

Kai Zhang

Key Laboratory of Dynamics and Control of
Flight Vehicle,
Ministry of Education,
School of Aerospace Engineering,
Beijing Institute of Technology,
Beijing 100081, China

Gengkai Hu¹

Key Laboratory of Dynamics and Control of
Flight Vehicle,
Ministry of Education,
School of Aerospace Engineering,
Beijing Institute of Technology,
Beijing 100081, China
e-mail: hugeng@bit.edu.cn

Wave-Based Control of a Crane System With Complex Loads

In the framework of wave-based method, we have examined swing motion control for double-pendulum and load-hoist models. Emphases are placed on wave scattering by the middle load mass in the double-pendulum model and on time-varying configuration in the load-hoist model. By analyzing wave transmission and reflection, trolley's motion to alleviate swing is designed by absorbing reflected wave through adjusting the velocity of trolley. Simulation and experiment are also conducted to validate the proposed control method. The results show that with the designed trolley's motion swings of load can be significantly reduced for both double-pendulum model, suspended rod model which is demonstrated a special case of double-pendulum model, and load-hoist model. Simulation results agree well with the experimental measurement. Launch velocity profiles may have important impact on motion design, especially on force necessary to displace trolley. Finally, a wave-based feedback control is also discussed to demonstrate the flexibility of method. [DOI: 10.1115/1.4036228]

1 Introduction

A typical task of crane is to displace load to a targeted position. Its performance can be measured under various headings, including minimization of sway during and at end of motion, tracking along a desired trajectory, accurate repositioning payloads within the shortest possible time, maximum repetition rate, and safety [1]. This problem in engineering is not well solved yet, and control performance is still depending on the experience of crane driver. Stable and high efficient control strategy is still demanding. To tackle this problem of position and vibration control, different methods have been proposed, which can be classified into two main categories: closed-loop control and open-loop control. Closed-loop control needs extra sensors to probe response of a dynamic system and uses it as feedback to define control strategy. This method is reliable and robust without detailed analysis on the dynamics of the system, and it is widely used in system control. Here, for our crane motion control problem, the objective is to examine influence of wave scattering in a system on control strategy, and an open-loop control is used because full understanding of the dynamics of system may be helpful. The most common approach to this problem is based on modal vibration control, and dynamics of payload and string are idealized as simple- or double-pendulum systems. Control strategy is proposed based on modal response of the system. For example, a widely used open-loop control for this problem is input-shaping method, proposed initially by Smith in the late 1950s [2], and three-dimensional (3D) pendulum and double-pendulum problems have also been examined lately [3–11].

In the modal control method, we have to truncate a finite number of modes to characterize and control the system [12]. This makes modal control method inadequate for large-scale flexible structure usually with crowded modes at low frequency. A large number of modes have to be considered to accurately characterize and control their responses. In the revision of this paper, we notice a recent work of Celentano [13]. This method allows the modeling of a flexible robot, also under the hypothesis of large link

deformations, with the essential methodology for rigid robots by subdividing fictitiously link of the robot into sublinks. On the other hand, for time-varying structures, such as deployable structure or gantry crane during lift of load, even modal concept is questionable. Vibration is the result of standing wave. Wave-based control method takes input as a disturbance traveling in a structure, and vibration of the structure will be alleviated if reflected wave is absorbed [14,15]. The first approach of this kind to crane motion problem was proposed by Saigo et al. [16]. A fictitious structure is supposed to link to the examined system, and it absorbs energy and eliminates in turn vibration by allowing wave to go into infinite space. Later, O'Connor developed a simple wave-based method to control motion of a gantry crane system [17]. The basic idea is to absorb reflected wave from load by adjusting velocity of the crane. Wave-based method is further extended to feedback controls [18,19]. However, these works are limited to simple structures, and wave scattering in structure is not considered. For complex structures, waves will be scattered due to impedance mismatch, e.g., presence of junctions, their impact on wave-based control is not thoroughly examined yet. In addition, application of wave-based method to time-variable structures is few, except Ref. [20], where a polynomial function is used for hoisting function and the control scheme is designed by using inverse dynamics instead of wave absorption.

In this paper, we will consider a crane system with emphasize on the following two problems: wave scattering by a junction and time-varying string length. Both theoretical analysis and experiment are conducted based on wave-based control method. The paper is organized as follows: In Sec. 2, fundamental ingredients of wave-based control method are first provided, then control strategies are derived for a double-pendulum and load-hoisting model. Detailed numerical simulation and experimental validation are provided in Sec. 3. In Sec. 4, different loading strategies are examined. Wave-based feedback control is discussed in Sec. 5. Finally, conclusions are given in Sec. 6.

2 Mathematical Modeling

2.1 Wave-Based Control Method. A gantry crane system is idealized as follows: A trolley, moving horizontally, is attached by a flexible string with a load mass, as illustrated in Fig. 1. In the

¹Corresponding author.

Contributed by the Dynamic Systems Division of ASME for publication in the JOURNAL OF DYNAMIC SYSTEMS, MEASUREMENT, AND CONTROL. Manuscript received October 21, 2015; final manuscript received January 11, 2017; published online June 1, 2017. Assoc. Editor: Douglas Bristow.

following analysis, the deformation and weight of string are neglected. The angular deflection of the string is assumed small so that the tension in the string equals to the weight of load mass $T = mG$, here G is the acceleration of gravity. The motions of the string and the load are characterized by wave equation and Newton's second law, respectively.

Wave equation of the string, in the hypothesis of small deformations, is given by

$$\rho \frac{\partial^2 y}{\partial t^2} - T \frac{\partial^2 y}{\partial x^2} = 0 \quad (1)$$

where y is the displacement of string from equilibrium position, and T and ρ are the tension force and density of the string, respectively. The corresponding boundary conditions are the velocity of trolley and load, which are given by $\dot{y}|_{x=0} = v_t$ and $\dot{y}|_{x=l} = w$.

Total horizontal force propagating in the string at location x and time t is derived by superposing two counter-propagating force waves $f(x - ct)$ and $g(x + ct)$ [17]

$$-T \frac{\partial y}{\partial x} = f(x - ct) + g(x + ct) \quad (2)$$

Local velocity of the string is given by

$$v = \frac{\partial y}{\partial t} = [f(x - ct) - g(x + ct)]/z \quad (3)$$

where $c = \sqrt{T/\rho}$ is the wave speed, and z is the wave impedance defined by $z = \rho c = \sqrt{\rho T} = T/c$.

Newton's second law of motion for load mass leads to

$$m\dot{w} = f(l - ct) + g(l + ct) \quad (4)$$

where m and w are the mass and velocity of the load, respectively, and l is the length of the string. The load is displaced from a static position, and then, the system equations can be solved. To dampen the swinging motion, the trolley speed should be controlled. The control strategy is to adjust the trolley speed so that it absorbs wave in the string arriving back to the trolley after reflection at the load and/or at discontinuity in the hanging system. If the trolley does not absorb this returning wave, it will be reflected back to the system, and swinging motion will take place. If, however, the trolley absorbs the returning wave and launches an incident

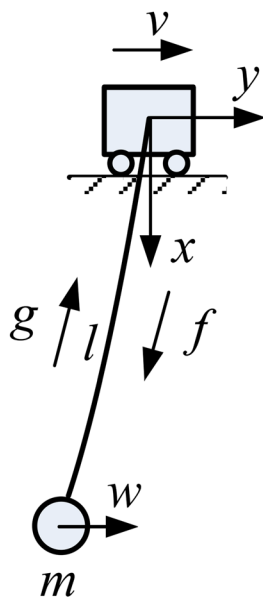


Fig. 1 Single load mass and uniform string model

wave, this launch wave will gradually accelerate the load without causing swing motion. The details of how this works will be explained below, and we will use $f = f(x - ct)$ and $g = g(x + ct)$ for simplification.

The trolley velocity v_t is assumed to have two parts: launch velocity v_l and absorb velocity v_a . The launch velocity v_l is used to generate incident wave and to accelerate the load, while the absorb velocity v_a is used to absorb reflected wave and to reduce swing of the load. The total trolley velocity is then given by

$$v_t = v_l + v_a \quad (5)$$

The absorb velocity is expressed as

$$v_a = -g|_{x=0}/z \quad (6)$$

When the launch velocity v_l starts from a constant velocity $v_l = v_0$, a force wave will propagate from the trolley to the load through the string. In the beginning, internal force in the string is only determined by the forward force wave f , since there is no reflected wave

$$f = v_0 z \quad (7)$$

When the force wave arrives at the load, it will accelerate the mass, and the motion of the load is determined by

$$m\dot{w} = f + g \quad (8)$$

$$wz = f - g \quad (9)$$

with the initial condition $w|_{t=l/c} = 0$, the velocity of the load is calculated by

$$w = 2v_0 \left(1 - e^{-\frac{z}{m}(t-l/c)}\right) \quad (10)$$

A reflected wave g will be generated from the load when it tends to move forward

$$g|_{x=l} = f - wz = 2v_0 z \left(e^{-\frac{z}{m}(t-l/c)} - \frac{1}{2}\right) \quad (11)$$

This reflected wave propagates from the load to the trolley, and when it arrives at the trolley, it can be evaluated by Eq. (11) simply by replacing t with $t - l/c$, that is,

$$g|_{x=0} = 2v_0 z \left(e^{-\frac{z}{m}(t-2l/c)} - \frac{1}{2}\right) \quad (12)$$

Therefore, by using Eq. (6), the wave to be absorbed is given by

$$v_a = v_0 - 2v_0 e^{-\frac{z}{m}(t-2l/c)} \quad (13)$$

Finally, the designed velocity of the trolley is written as

$$v_t = \begin{cases} v_0 & , 0 \leq t < 2l/c \\ 2v_0 \left(1 - e^{-\frac{z}{m}(t-2l/c)}\right) & , t > 2l/c \end{cases} \quad (14)$$

It is seen from Eqs. (10) and (14) that the velocities of the trolley and the load are almost same and the difference approaches zero with increasing time, which means the load follows quite well the motion of the trolley without swing, as shown in Fig. 2(a). This feature leads to the velocity of load change smoothly, which is completely different from input shaping. Input shaping is the most used open-loop control method for precise position control nowadays. It can realize rest to rest motion, but seldom concern about the swing during motion. Input shaping makes use of addition of

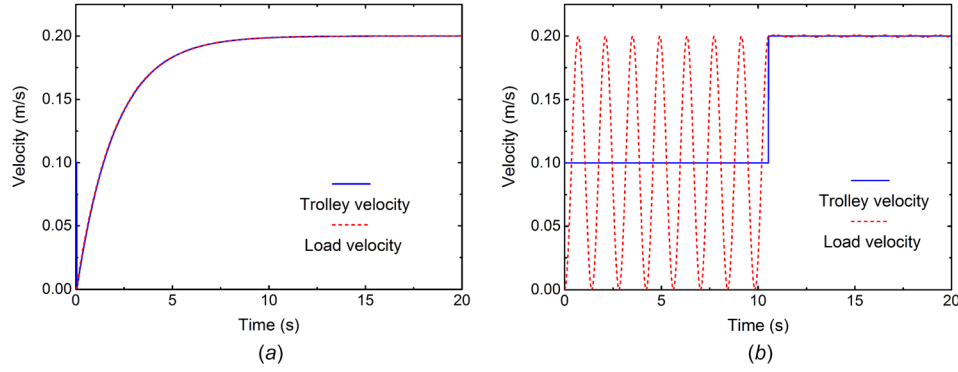


Fig. 2 Wave-based control (a) and input shaping (b) for simple pendulum

two input signal, it absorbs the energy when the second signal input into the system. Figures 2(a) and 2(b) show the difference of velocity changes of these two control methods for simple pendulum model. For input shaping in Fig. 2(b), the first step of velocity leads the motion of trolley, meanwhile causes dramatic vibration of load. The oscillation of load velocity will be eliminated until the second input step.

For the deceleration process, a simple way to break down load is time-reversal of the start-up motion, it is able to suppress swing of load at the end of operation [17]. Hence, in this case, only control strategy of the accelerating process is considered.

2.2 Double-Pendulum Model. For a double-pendulum system (Fig. 3), incident wave will be reflected and transmitted when it reaches the midload mass (load mass 1), mass 1 is therefore accelerated. The transmitted wave will accelerate in turn load mass 2 and be reflected back. The wave traveling process is much more complex than that in the single pendulum system, but the basic principle remains the same, i.e., absorbing the reflected wave at the trolley to alleviate swing motion. According to equilibrium equation and continue condition of the velocity at the middle mass, the motion of load 1 is determined by

$$m_1 \dot{w}_1 = f_1(x_1 - c_1 t) + g_1(x_1 + c_1 t) - f_2(x_1 - c_2 t) - g_2(x_1 + c_2 t) \quad (15)$$

$$w_1 = (f_1(x_1 - c_1 t) - g_1(x_1 + c_1 t))/z_1 \\ = (f_2(x_1 - c_2 t) - g_2(x_1 + c_2 t))/z_2 \quad (16)$$

where f_i and g_i are the forward and backward waves in the string i ($i = 1, 2$), respectively. c_i and z_i are the wave speeds and impedances in the string i , and w_i is the velocity of the load i .

The motion of load 2 is provided by solving the following equations:

$$m_2 \dot{w}_2 = f_2(x_2 - ct) + g_2(x_2 + ct) \quad (17)$$

$$w_2 = (f_2(x_2 - ct) - g_2(x_2 + ct))/z_2 \quad (18)$$

In the following, we still consider the case of a constant launch velocity $v_l = v_0$, i.e., $f_1 = v_0 z_1$. To design trolley velocity, we consider an incident wave that is excited from the trolley and travels into the system. t_1 is defined as the time needed for wave to travel through the upper string which is $t_1 = l_1/c_1$, and t_2 is defined as the corresponding time of the lower string which is $t_2 = l_2/c_2$. At time t_1 , the front of the force wave first reaches load 1, and at this moment, no wave is reflected back from load 2, i.e., $g_2 = 0$. So, the motion of m_1 at time interval $[t_1, t_1 + 2t_2]$ is given by

$$m_1 \dot{w}_1 + (z_1 + z_2)w_1 = 2f_1 \quad (19)$$

And with the initial condition $w_1(t_1) = 0$, we get

$$w_1 = \frac{2v_0 z_1}{z_1 + z_2} - \frac{2v_0 z_1}{z_1 + z_2} e^{-\frac{z_1 + z_2}{m_1}(t - t_1)} \quad (20)$$

According to Eqs. (15) and (16), we derive the reflected and the transmitted waves at load 1

$$g_1 = f_1 - w_1 z_1 = \frac{v_0 z_1 (z_2 - z_1)}{z_1 + z_2} + \frac{2v_0 z_1^2}{z_1 + z_2} e^{-\frac{z_1 + z_2}{m_1}(t - t_1)} \quad (21)$$

$$f_2 = w_1 z_2 = \frac{2v_0 z_1 z_2}{z_1 + z_2} - \frac{2v_0 z_1 z_2}{z_1 + z_2} e^{-\frac{z_1 + z_2}{m_2}(t - t_1)} \quad (22)$$

When the reflected wave g_1 reaches the trolley, it is absorbed by defining the absorb velocity of the trolley as $v_a = -g_1/z_1$, so the designed trolley velocity is $v_l + v_a = v_0 - g_1/z_1$.

At the time $t_1 + t_2$, the transmitted wave f_2 reaches load 2 and speeds it up. The motion equation of m_2 at time interval $[t_1 + t_2, t_1 + 3t_2]$ is given by

$$m_2 \dot{w}_2 + z_2 w_2 = 2f_2 \quad (23)$$

And with the initial condition $w_2(t_1 + t_2) = 0$, we have

$$w_2 = \frac{4v_0 z_1}{z_1 + z_2} - \frac{4m_1 v_0 z_1 z_2}{(m_1 z_2 - m_2(z_1 + z_2))(z_1 + z_2)} e^{-\frac{z_1 + z_2}{m_1}(t - t_1 - t_2)} \\ + \left(\frac{4m_1 v_0 z_1 z_2}{(m_1 z_2 - m_2(z_1 + z_2))(z_1 + z_2)} - \frac{4v_0 z_1}{z_1 + z_2} \right) e^{-\frac{z_2}{m_2}(t - t_1 - t_2)} \quad (24)$$

In turn, a reflected wave from load 2 is generated

$$g_2 = f_2 - w_2 z_2 = -\frac{2v_0 z_1 z_2}{z_1 + z_2} \\ + \frac{2v_0 z_1 z_2 (m_1 z_2 + m_2(z_1 + z_2))}{(m_1 z_2 - m_2(z_1 + z_2))(z_1 + z_2)} e^{-\frac{z_1 + z_2}{m_1}(t - t_1 - t_2)} \\ - \frac{4m_2 v_0 z_1 z_2}{m_1 z_2 - m_2(z_1 + z_2)} e^{-\frac{z_2}{m_2}(t - t_1 - t_2)} \quad (25)$$

When the reflected wave g_2 reaches load 1, the motion equation of m_1 changes to

$$m_1 \dot{w}_1 + (z_1 + z_2)w_1 = 2(f_1 - g_2) \quad (26)$$

By solving this equation, the velocity of load 1 in the time period from $t_1 + 2t_2$ to $t_1 + 4t_2$ can be known. Repeating the processes by solving the motion equations of m_1 and m_2 alternately, the

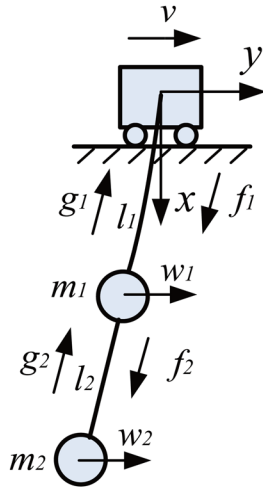


Fig. 3 Double-pendulum model

velocity of both loads will be obtained. The velocity of the trolley is designed by absorbing the reflected wave each time as $v_r = v_l - g_1/z$, and the swing of both loads can be eliminated remarkably. Here, g_1 will include the reflected wave directly from load 1 and the wave reflected from load 2 and transmitted through load 1 as well.

Finally, it is interesting to note that a rigid rod connected to the trolley by a flexible string is a special case of the examined double-pendulum model. Consider, for example, a rigid-rod system in Fig. 4, when writing down equation of motion (given in the Appendix), it is easily found that the motion equation of the rigid-rod model is exactly the same as that of the double-pendulum model with the following rescaled parameters:

$$l'_1 = l_1, l'_2 = 2l_2/3, m_1 = m_2/3 \quad (27)$$

where the primed quantity refers to the equivalent one in the double-pendulum model. So, the control strategy of a double-pendulum model can be used directly in a rigid-rod system with the rescaled parameters.

2.3 Load-Hoist Model. In this section, we will consider a simple pendulum system moving horizontally with the same time load height control, as shown in Fig. 5. The change of string

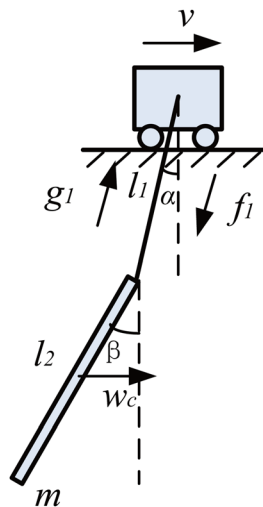


Fig. 4 A rigid-rod model

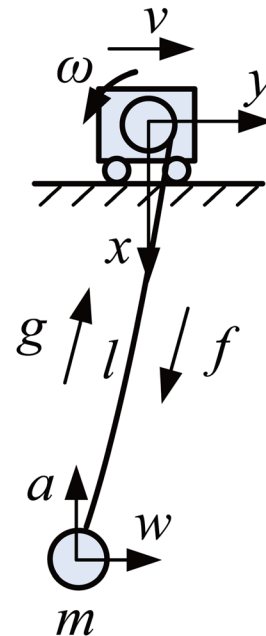


Fig. 5 Hoisting load model

length alters the natural frequency of the system, and in terms of wave propagation, only wave traveling time between the trolley and the load needs to be modified. So, the hoisting load model may be derived from a single pendulum model by modifying wave traveling time in each time increment. As the geometry of this model is not symmetric, deceleration process could not be derived by time-reversal of the acceleration process. The load will be decelerated by setting the launch velocity to be zero and absorbing continually the reflected waves.

To design the trolley velocity in the acceleration process, the launch velocity v_l starts from a constant velocity v_0 , and at the same time, the load mass moves upward with a speed a . Here, for simplicity, a is assumed constant. The force wave propagates from the top of the string to the bottom, since there is no reflected wave g at the beginning, and the internal force in the string is given by $f = v_0 z$. At the time $t_1 = l/c$, the force wave arrives at the load and accelerates it, and the velocity of the load mass is still characterized by Eqs. (8) and (9). With the initial condition $w(t_1) = 0$, the velocity of the load in the entire acceleration process can be calculated as

$$w = 2v_0(1 - e^{-\frac{z}{m}(t-t_1)}) \quad (28)$$

With further move of the load, a reflected wave from the bottom will be generated as

$$g = f - wz = 2v_0 z \left(e^{-\frac{z}{m}(t-t_1)} - \frac{1}{2} \right) \quad (29)$$

The reflected wave travels from the bottom load to the top trolley and the length of the string gets shorter at the same time. So, at time $t_2 = (c-a)l/(c+a)c$, the reflected wave arrives at the top trolley, and it is written as

$$g = 2v_0 z \left(e^{-\frac{z}{m}(t-t_2)} - \frac{1}{2} \right) \quad (30)$$

The absorb velocity for this reflected wave from $t = t_2$ is given by using Eq. (6)

$$v_a = -g/z = v_0 - 2v_0 e^{-\frac{z}{m}(t-t_2)} \quad (31)$$

So, the total velocity of the trolley in the entire acceleration process should be

$$v_t = \begin{cases} v_0 & , 0 \leq t < t_2 \\ 2v_0 - 2v_0 e^{-\frac{z}{m}(t-t_2)} & , t \geq t_2 \end{cases} \quad (32)$$

To decelerate the load, the launch velocity v_l is removed, for example, at a given time t_3 . Without new force wave entering the string, the entire system will come gradually to rest due to the absorption. To derive the necessary velocity of the trolley in this deceleration process, we consider the incident wave arriving at the load at time $t_4 = t_3 + (l - at_3)/c$. The motions of Eqs. (8) and (9) of the load lead to

$$m \frac{dw}{dt} + zw = 0 \quad (33)$$

And with the following initial condition:

$$w(t_4) = 2v_0(1 - e^{-\frac{z}{m}(t_4-t_1)}) \quad (34)$$

The velocity of the load is derived as

$$w = 2v_0(1 - e^{-\frac{z}{m}(t_4-t_1)})e^{-\frac{z}{m}(t-t_4)} \quad (35)$$

According to Eq. (3), the reflected wave is given by

$$g|_{x=l-at_4} = -2v_0z(1 - e^{-\frac{z}{m}(t_4-t_1)})e^{-\frac{z}{m}(t-t_4)} \quad (36)$$

At time $t_5 = (l - at_4)/(c + a) + t_4$, this reflected wave arrives at the top trolley, and it is written as

$$g|_{x=0} = -2v_0z(1 - e^{-\frac{z}{m}(t_4-t_1)})e^{-\frac{z}{m}(t-t_5)} \quad (37)$$

So, the absorb velocity is determined by

$$v_a = 2v_0(1 - e^{-\frac{z}{m}(t_4-t_1)})e^{-\frac{z}{m}(t-t_5)} \quad (38)$$

As the launch velocity is removed, the designed velocity of the trolley is equal to the absorb velocity. So, the velocity of the trolley in the deceleration process should be

$$v_t = \begin{cases} v_0 - 2v_0 e^{-\frac{z}{m}(t-t_2)} & , t_3 \leq t < t_5 \\ 2v_0 \left(1 - e^{-\frac{z}{m}(t_4-t_1)}\right) e^{-\frac{z}{m}(t-t_5)} & , t \geq t_5 \end{cases} \quad (39)$$

3 Simulation and Experiment

In this section, we will illustrate the efficiency of the proposed method in Sec. 2 through numerical examples and compare them with experiments. In the experiment, the string with a load is mounted on a line guided track, driven by a stepper motor. The velocity of the trolley is controlled by rotation speed of motor and the displacement of the load is measured by laser displacement sensors. The material and geometric parameters are as follows: the density of the cotton string is $\rho = 6.2 \times 10^{-4}$ kg/m, the masses of the loads are $m_1 = m_2 = 0.005$ kg, $l_1 = l_2 = 0.25$ m for the segments of the string in the double-pendulum model, $m = 0.057$ kg, $l_1 = 0.51$ m, and $l_2 = 0.205$ m in the rigid-rod model, $m = 0.0135$ kg, and the initial length of the string $l = 0.62$ m in the load-hoist model.

3.1 Double-Pendulum Model. In the simulation and experiment, a double pendulum is displaced by a motor from rest to a displacement $d = 0.588$ m during a period of time 12 s, the velocity of the trolley is designed based on the wave-based control

method explained previously, and the launch velocity is 0.03 m/s. The displacement and velocity are set according to the length of line guide track available in the experiment, which are different from real crane applications, but the principle holds for large launch velocity. In simulation, the pendulum models are built in commercial finite element software ANSYS using the link and mass elements, and the control signal is applied under a series of time steps. Figure 6 shows the analytical and finite element results of displacement (a) and velocity (b) for load 2 as a function of time when the trolley moves following the designed velocity. It is seen from the analytical result that load 2 follows closely the motion of the trolley and moves with little swing, and its velocity fluctuates a little at beginning and converges toward the target velocity profile, i.e., the velocity profile of the trolley, with reducing swing motion. The numerical displacement of load 2 follows well with the analytical result. Some errors accumulated in load velocity as the load velocity is divided into discontinuous load step in numerical calculation. Here, only the acceleration process is considered, and the deceleration process can be obtained by time-reversal technique, not shown in the figure.

Figure 7 illustrates the computed force on load 2 for a period time of 10 s (acceleration process), it is seen that both incident force wave f_2 and reflected force wave g_2 quickly decay out at the end of the acceleration process, so as the total force $f_2 + g_2$.

To validate the model, experimental measurement is also conducted, as shown in Fig. 8. The displacement of load as a function of time is measured by laser displacement sensors, and the velocity of the load can be then obtained. In the experiment, the launch velocity is taken the same as in the simulation $v_l = 0.03$ m/s. For comparison, we also analyzed the case where the trolley moves at a constant velocity $v_c = 0.049$ m/s, this velocity is chosen in order to make the same displacement in the same period of time as in the controlled motion, so two motions have the same average velocity. Figure 9(a) shows the comparison of the displacement of load 2 as a function of time for the cases where the trolley follows the designed velocity and the constant velocity in experiment. Figures 9(b) and 9(c) show the simulation and experiment of the velocity of load 2 in the designed velocity case and the constant velocity case, respectively.

Compared to the constant velocity case, the load moves and stops at end without significant swing when following the designed motion. In the constant velocity motion, a large acceleration is needed at the beginning to accelerate the trolley to the desired velocity. This will induce the observed large swing motion. The predicted responses of load agree well with the measurement, as shown in Fig. 9.

Finally, a gantry crane with a suspended rigid rod is also analyzed to reduce the swing motion of the rod. The rigid rod is displaced from rest to a displacement 0.525 m during a time 7 s. The launch velocity $v_l = 0.1$ m/s is taken in the designed motion. A constant velocity loading case is also considered for comparison, in which the velocity of the trolley is adjusted to be $v_c = 0.08$ m/s. Figure 10 shows the comparison result of the displacements at the bottom end of the rod for the constant velocity motion and the wave-controlled motion, respectively. The proposed control strategy reduces efficiently the swing of the rigid rod during displacement, and the swing amplitude at the arrival decreases from 31.76 mm of the constant velocity motion case to 4.27 mm in the proposed control motion. Again, the simulation agrees well with the experiment.

3.2 Load-Hoist Control. In this section, we will consider the load-hoist model discussed previously. The load is displaced from rest to a horizontal distance of 0.585 m, and at the same time, it is hoisted at a constant velocity $a = 0.06$ m/s for a period of time 7.5 s. To design the motion, the launch velocity is set to be 0.05 m/s, and a constant velocity (horizontal) motion $v_c = 0.078$ m/s is also examined for comparison. In the experiment, a rotational motor is used to lift the load in addition to a stepper

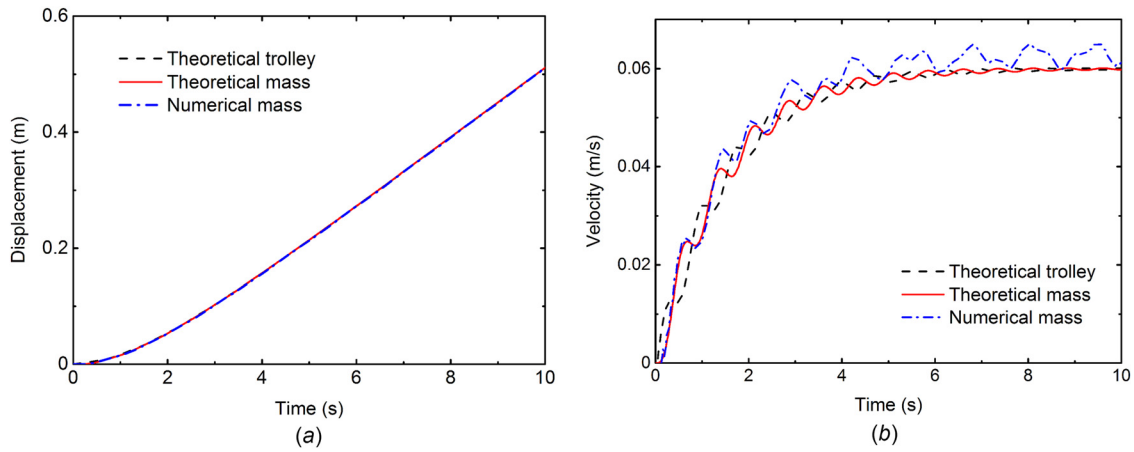


Fig. 6 Analytical and finite element results of displacement (a) and velocity (b) as a function of time for double-pendulum model

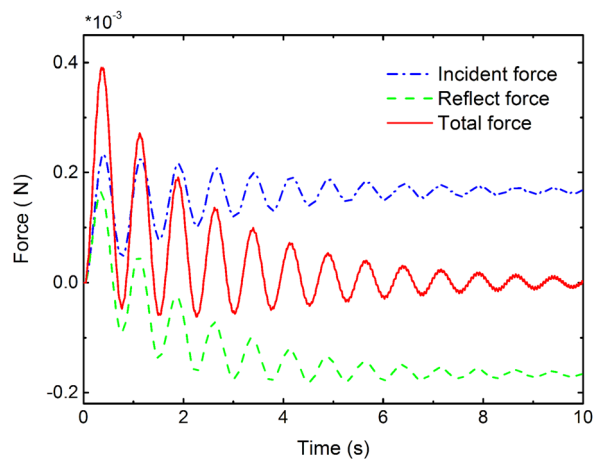


Fig. 7 Simulation of force variation on load 2 in double-pendulum model

motor providing a horizontal motion, and the experimental setup is shown in Fig. 11.

Figure 12 shows the corresponding measurements for displacement and velocity of the load. It is seen that the load moves smoothly and stops with little swing with the proposed control motion, and the amplitude of swing drops from 52.04 mm to

2.84 mm, compared to a constant velocity motion. It is also interesting to note from the velocity variation that the frequency increases due to the shortening string length, and the swing of the load is significant if without control.

4 Influence of Launch Velocity

In the previous motion design discussed in Sec. 2.1, the launch velocity is taken constant, as initially proposed by O'Connor [17]. The constant launch velocity will rapidly accelerate the load; however, the velocity of the trolley needs quickly to be dropped to nearly zero at the beginning to avoid large swing of the load. To circumvent this problem, different forms of the launch velocity can be assumed to design velocity profile of the trolley. In this section, we will examine the influence of launch velocity on the designed velocity profile of the trolley. In the following, we consider only a single pendulum system, moving horizontally with the parameters $l = 0.5$ m, $m = 0.4$ kg, and $\rho = 1 \times 10^{-2}$ kg/m.

For the first example, the launching velocity is assumed to follow an exponential form of $v_l = v_0(1 - e^{-z/m})$, where z and m are the impedance and mass, respectively. This profile will make the velocity converge to a constant value, which is easy to meet maximum velocity required in engineering and also easy to make a deceleration through velocity reversal. The incident force wave is given by $f = v_l z = v_0 z(1 - e^{-z/m})$. By solving the motion equations $m\dot{w} = f + g$ and $wz = f - g$, the velocity of the load is expressed as

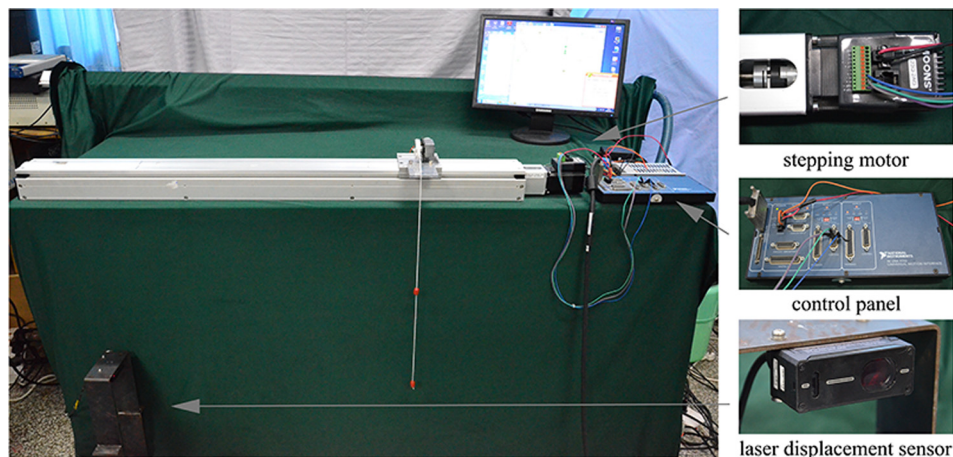


Fig. 8 Experimental setup for double-pendulum model

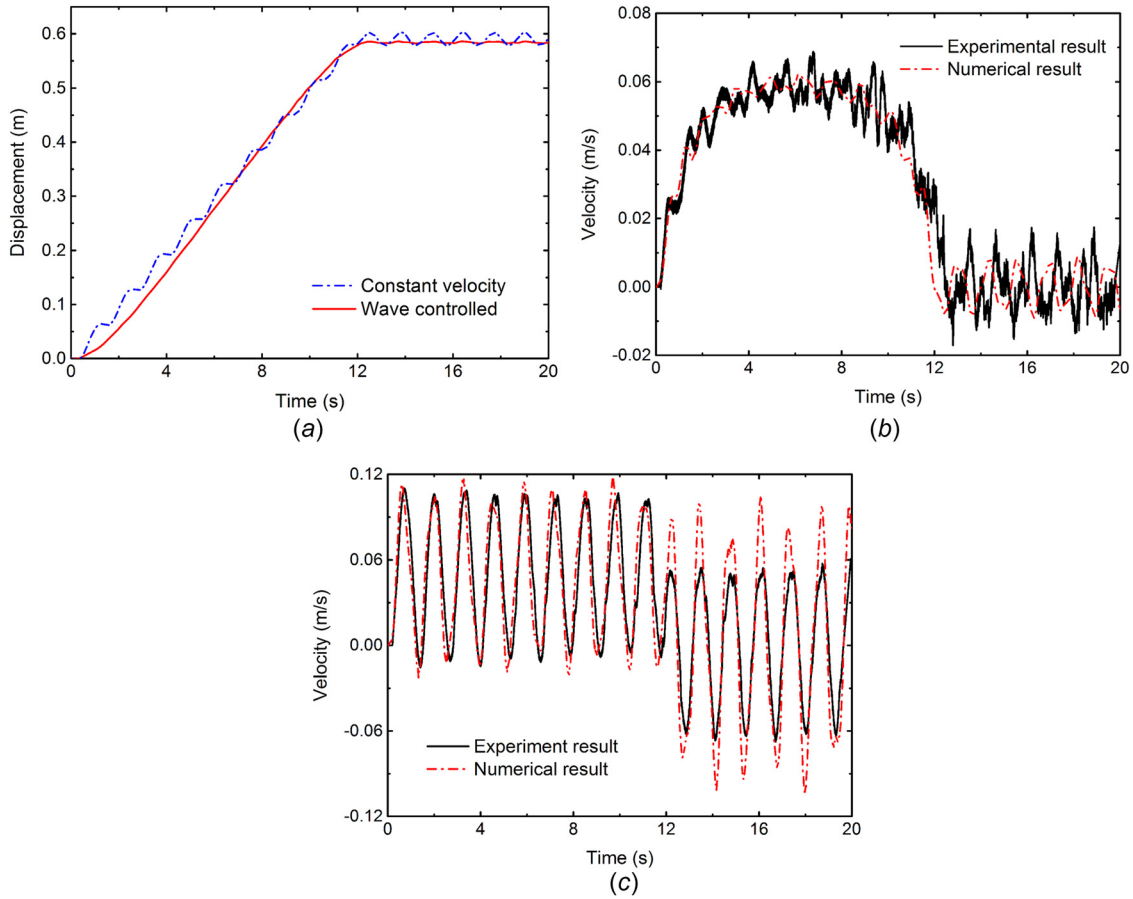


Fig. 9 Comparison between simulation and experiment for displacement and velocity of load 2 in double-pendulum model: (a) experimental displacements in wave-controlled case and constant velocity case, (b) velocity variation in the wave-controlled case, and (c) velocity variation in constant velocity case

$$w = 2v_0(1 - e^{-z(t-t_c)/m}) - \frac{2v_0z}{m}(t - t_c)e^{-z(t-t_c)/m} \quad (40)$$

where $t_c = l/c$ is the wave traveling time in the string. The acceleration of the load is obtained as

$$\dot{w} = \frac{2v_0z^2}{m^2}(t - t_c)e^{-\frac{z(t-t_c)}{m}} \quad (41)$$

According to the wave-based method, the designed velocity of the trolley is written as by absorbing reflected wave

$$v_t = 2v_0 - v_0e^{-z/m} - v_0(1 - e^{-z(t-2t_c)/m}) - \frac{2v_0z}{m}(t - 2t_c)e^{-z(t-2t_c)/m} \quad (42)$$

The acceleration of the trolley is given by

$$a_t = \frac{v_0z}{m}e^{-\frac{z}{m}} + \left[\frac{2v_0z^2}{m^2}(t - 2t_c) - \frac{v_0z}{m} \right] e^{-\frac{z(t-2t_c)}{m}} \quad (43)$$

For the second example, the launch velocity of the trolley is assumed to follow a trapezoid form, i.e., a velocity with constant

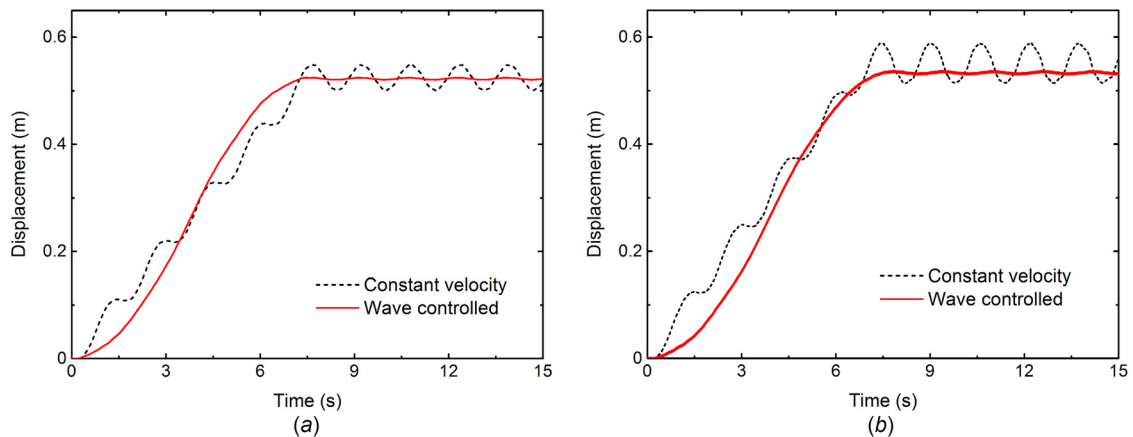


Fig. 10 Displacement of rigid rod (the bottom end) for constant velocity motion and wave-controlled motion: (a) simulation and (b) experiment

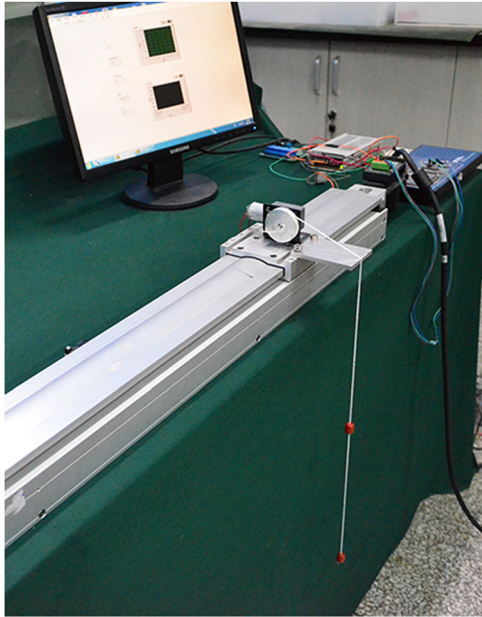


Fig. 11 Experimental setup for load-hoist model

acceleration of $v_l = a_0 t$ from the period of 0 to t_1 and then followed by a constant speed $v_l = a_0 t_1$. For the period of the constant acceleration, the incident force wave is given by $f = v_l z = a_0 z t$. By solving the motion equations $m\dot{w} = f + g$ and $wz = f - g$, the load velocity is derived as

$$w = \frac{2ma_0}{z} e^{-\frac{z}{m}(t-l/c)} + 2a_0(t-l/c) - \frac{2ma_0}{z} \quad (44)$$

The designed velocity of the trolley is provided by

$$v_t = \frac{2ma_0}{z} (e^{-\frac{z}{m}(t-2l/c)} - 1) + 2a_0(t-l/c) \quad (45)$$

According to the trolley velocity, the acceleration of the trolley is written as

$$a_t = 2a_0(1 - e^{-\frac{z}{m}(t-l/c)}) \quad (46)$$

Figure 13 shows the designed trolley velocity profile (a) and the finite element simulation of the load response (b) according to the different launch velocity functions, including constant, exponential,

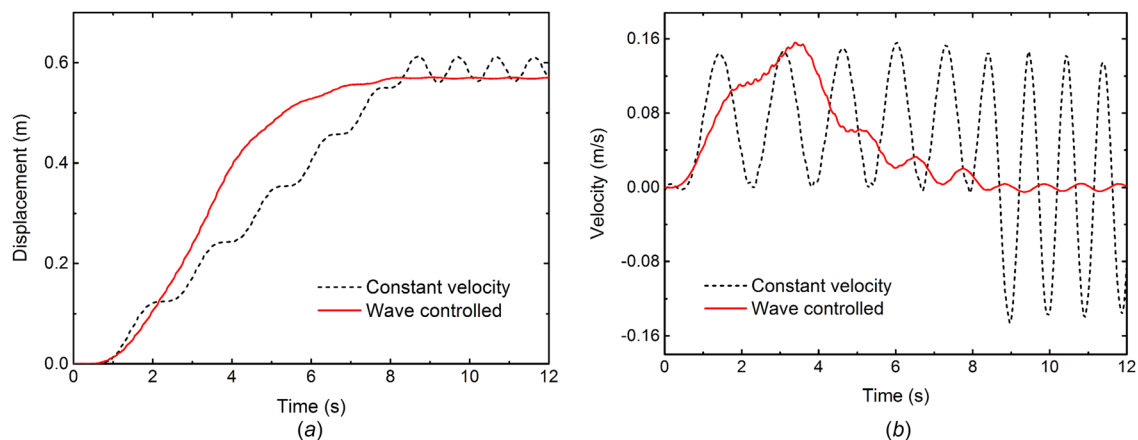


Fig. 12 Comparison of measured horizontal displacement (a) and velocity (b) of load for constant velocity motion and proposed control motion

and trapezoid forms. The launch velocity of the constant form provides a rapid increase in velocity, but will in turn induce a large acceleration. Compared with the constant launch velocity case, the launch velocity of the exponential form shows a slower and smoother increase in velocity, therefore avoid velocity jump. The load response in the case of the launch velocity of the trapezoid form manifests a little swing due to the switch of the acceleration.

Force acting on the trolley depends intimately on its velocity variation. Figure 14 illustrates the acceleration profiles of the trolley (a) and the load (b) for different launch velocity profiles. It is found that the accelerations of the trolley and the load mass of the exponential and trapezoid profile inputs are much smaller than those in the constant velocity one, hence smaller force will be induced in the string. The trapezoid form velocity input will trigger swing motion and cause acceleration oscillation, as shown in Fig. 14(b).

Wave-based control method is based on the analytical solutions of wave equations. If errors of geometry and material parameters exist in the structures, the control strategy will result in residual vibration. Natural frequencies of structures depend on the parameters of geometry and materials. In order to confirm the sensitivity of wave-based control with respect to model and parameter uncertainties, errors of natural frequency are induced to evaluate the change of amplitudes of residual vibration. Figure 15 shows the amplitudes of residual vibration as a function of errors of natural frequency in different launch velocity inputs. The results are gotten by the numerical results of the simple pendulum model under different forms of launch velocity input. It can be seen that the vibration percentage increases linearly with the increase of frequency error. But for different input control strategy, the levels of residual vibration amplitude vary a lot. The exponential input control strategy is robust. Even the frequency error is as large as 0.25, its vibration percentage is still under 0.6%, which is much better than the uniform velocity control strategy. The vibration percentage reaches 5% when the frequency error is 0.25.

5 Wave-Based Feedback Control Model

Wave-based method explained previously is not only limited to define open-loop control strategy but also can be used to design feedback control as well, which may be more simple and robust. By implementing an additional sensor to measure the velocity of load and inclined angle of the string, instead of analytical derivation as in the case of the open-loop control, a feedback control strategy can be defined by adjusting trolley's velocity through absorption of reflected wave. In this section, we will provide two simple examples to illustrate basic idea of wave-based feedback control without consideration of delay of feedback.

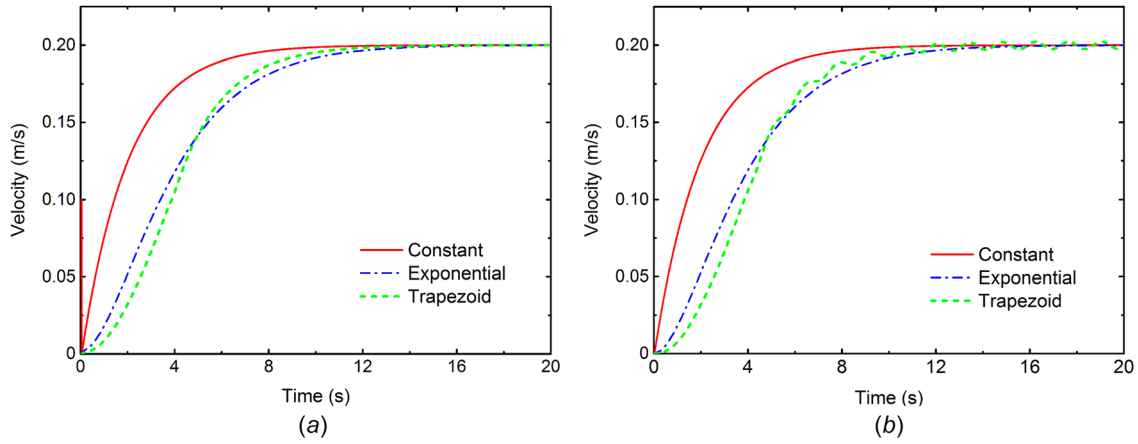


Fig. 13 Comparison of different designed velocity profiles of the trolley (a) and responses of the load (b) for different launch functions, including constant, exponential, and trapezoid forms

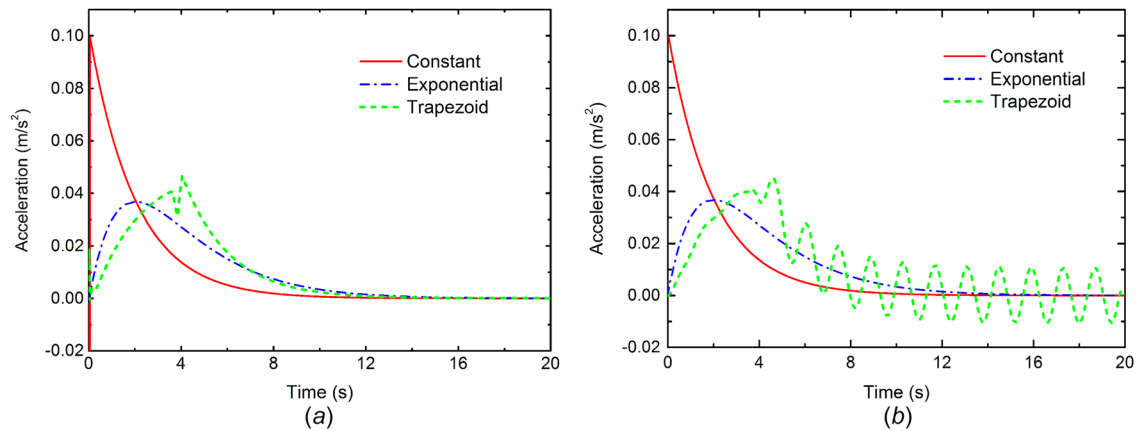


Fig. 14 Acceleration profiles of trolley (a) and load (b) for different launch velocity profiles, including constant, exponential, and trapezoid forms

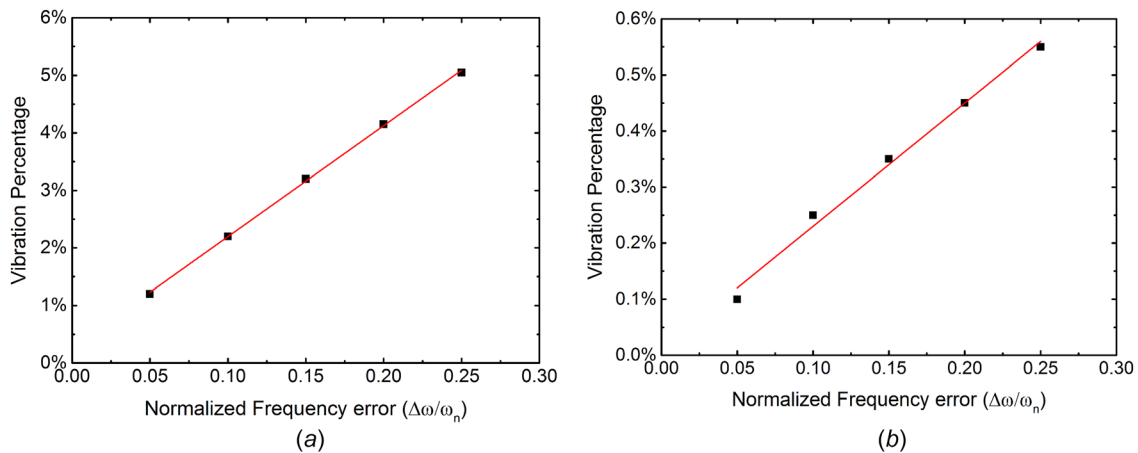


Fig. 15 Vibration amplitude changes with the normalized frequency error in constant (a) and exponential (b) launch velocity control method

According to Eqs. (2) and (3), two counter-propagating force waves can be obtained according to the velocity v at each point on the string and string tilt angle $\theta = \partial y / \partial x$

$$f(x - ct) = \left(v_z - T \frac{\partial y}{\partial x} \right) / 2 \quad (47)$$

$$g(x + ct) = - \left(v_z + T \frac{\partial y}{\partial x} \right) / 2 \quad (48)$$

The feedback velocity is set to generate a desired incident wave and to absorb the reflected wave. With the help of velocity of trolley v_t and the string tilt angle at the trolley end θ_t , the launch

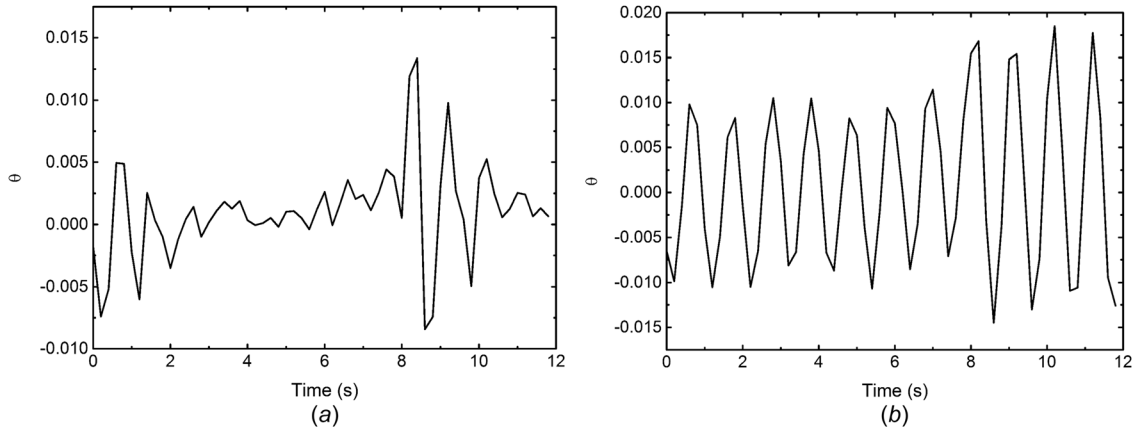


Fig. 16 Swing of load for a single pendulum: (a) with control and (b) without control

velocity v_l and absorb velocity v_a can be derived to satisfy the requirement of the incident and reflected waves.

If controller keeps launch wave constant, the launch velocity is derived in this case as

$$\left(v_l z - T \frac{\partial y}{\partial x}\right) / 2 = v_c z \quad (49)$$

$$v_l = 2v_c + T\theta_l / z \quad (50)$$

Absorb velocity is derived by absorbing reflected wave

$$v_a z = g(x + ct) = -\left(v_l z + T \frac{\partial y}{\partial x}\right) / 2 \quad (51)$$

$$v_a = -v_l / 2 - T\theta_l / 2z \quad (52)$$

Total velocity of the designed feedback control is to sum up the launch velocity (Eq. (50)) and the absorb velocity (Eq. (52)), i.e., it is obtained by adding a feedback of velocity and a feedback of tilt angle of string on a constant velocity

$$v'_l = v_l + v_a = 2v_c - v_l / 2 + T\theta_l / 2z \quad (53)$$

Particularly, if the launch wave f is set to zero, this method can alleviate initial vibration by absorbing reflected wave as well

$$v'_l = v_a = -v_l / 2 - T\theta_l / 2z \quad (54)$$

In order to validate the proposed feedback control strategy, we use two laser displacement sensors to measure the velocity of load and the string tilt angle during motion. To make a feedback, the

trolley's velocity is calculated and applied for a given time increment step-by-step. In the first step, a constant velocity v_c of the trolley is set. When the trolley moves, the velocity of load and the string tilt angle are measured, and they are used to evaluate the velocity for the next step according to Eq. (53). This process repeats until the trolley stops and the load mass comes to rest. Two examples are analyzed, vibration control for a simple pendulum for a given distance which is controlled by adding the feedback, and the other is vibration suppression for single and double pendulums with initial swing motion. The parameters of the double pendulum are the same as previously discussed in Sec. 3.

For the constant velocity with feedback control motion of a single pendulum, the constant velocity is set to be $v_c = 0.015$ m/s and keeps for 8 s, which makes the trolley move over a distance of 0.12 m. The feedback control time increment is set to 0.2 s. From the beginning, the tilt angle of string is measured and the velocity of trolley is calculated for the next step 0.2 s. Then, the entire process repeats itself with velocity updated in real-time. The delay of 0.2 s in the feedback will induce the load to swing for some cycles before catching up with speed of trolley. Swing of load during motion and stop is given in Fig. 16(a), and that of the load without control is also illustrated in Fig. 16(b) for comparison. It is found indeed that swing of load is reduced rapidly with the wave-based feedback control strategy.

The second example is control of initial swing of single and double pendulums with wave-based feedback control method. The trolley remains at rest but with initial swing motion of the load. In this case, the launch velocity equals to zero; and the velocity of trolley is adjusted by the absorb velocity with consideration of feedbacks from the trolley velocity and the tilt angle in real-time (Eq. (54)). Figures 17(a) and 17(b) show the experimental results for the single

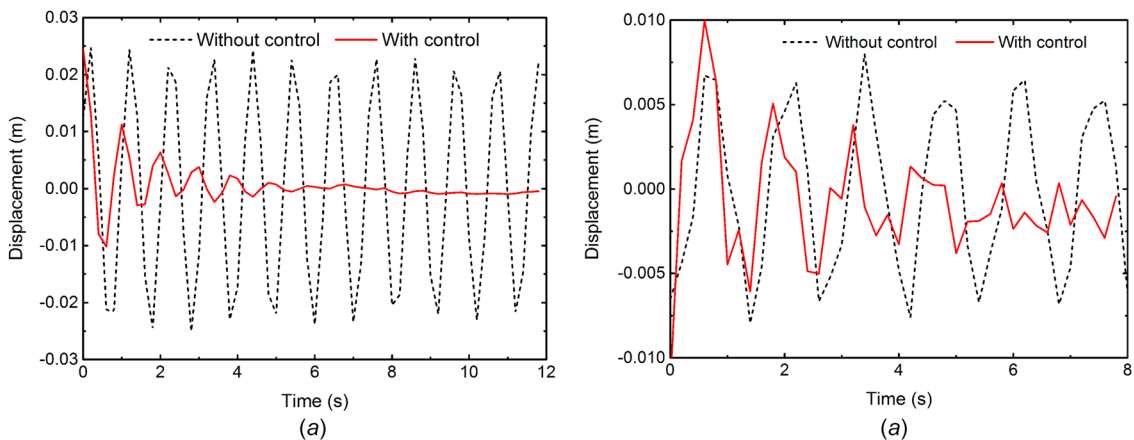


Fig. 17 Swing of pendulum with and without control: (a) single pendulum and (b) double pendulum

and double pendulums with and without controls, respectively. Again, the initial swing motions are rapidly attenuated both for single and double pendulums with the proposed control strategy.

6 Conclusions

Wave-based open-loop control strategies are examined for gantry crane motion to reduce swing of loads, and double-pendulum and load-hoist models are considered with the objective to examine the wave scattering and configuration change with the wave-based method, respectively. In the analysis of the double-pendulum model, wave reflection and transmission in the system were analyzed. The gantry crane motion is determined by absorbing both reflected waves from the midload mass and end-load mass through adjustment of trolley velocity. The numerical simulation demonstrates high efficiency for swing motion alleviation, and the experimental measurement is also conducted to validate the proposed control strategy. It is also found that the suspended rigid-rod model can be derived as a special case of the double-pendulum model. In the load-hoist model, although the string length changes during the displacement of trolley, this can be simply taken into account by modifying the wave traveling time in a single pendulum model. The experiment is performed to validate this model. We also show that the launch velocity profiles may have important influence on the motion design, particularly on the peak force to move the trolley. Finally, wave-based feedback control is also discussed to demonstrate the power of this method.

Acknowledgment

This work was supported by the National Natural Science Foundation of China (Grant Nos. 11472044, 11290153, and 11221202).

Appendix: Rigid-Rod Model

The rigid-rod model is shown in Fig. 3, the trolley moves horizontally, and the rod motion is restricted to a plane, we use two angles α and β to characterize its motion. The potential energy and the kinetic energy of the load are written as

$$V = mg \left[\left(l_1 + \frac{l_2}{2} \right) - \left(l_1 \cos \alpha + \frac{l_2}{2} \cos \beta \right) \right] \quad (\text{A1})$$

$$T = \frac{1}{2} m v_{\text{center}}^2 + \frac{1}{2} I_{zz} \dot{\beta}^2 \quad (\text{A2})$$

where v_{center} is the velocity of the mass center of the rod, and I_{zz} is the rotation inertia related to the center. The Lagrangian of the system can be written as

$$\begin{aligned} L = \frac{1}{2} m \left[v^2 + l_1^2 \dot{\alpha}^2 + \frac{l_2^2}{4} \dot{\beta}^2 + 2l_1 v \cos \alpha \dot{\alpha} + l_2 \dot{x}_0 \cos \beta \dot{\beta} \right. \\ \left. + l_1 l_2 (\sin \alpha \sin \beta + \cos \alpha \cos \beta) \dot{\alpha} \dot{\beta} \right] \\ + \frac{1}{24} m l_2^2 \dot{\beta}^2 - m g l_1 (1 - \cos \alpha) - m g \frac{l_2}{2} (1 - \cos \beta) \end{aligned} \quad (\text{A3})$$

According to Lagrange equation, the motion equation of the rod can be derived

$$\begin{cases} m l_1^2 \ddot{\alpha} + m l_1 \cos \alpha \ddot{x}_0 + \frac{1}{2} m l_1 l_2 (\sin \alpha \cos \beta - \cos \alpha \sin \beta) \ddot{\beta}^2 \\ + \frac{1}{2} m l_1 l_2 (\sin \alpha \sin \beta + \cos \alpha \cos \beta) \ddot{\beta} + m g l_1 \sin \alpha = 0 \\ \frac{1}{3} m l_2^2 \ddot{\beta} + \frac{1}{2} m l_2 \cos \beta \ddot{x}_0 + \frac{1}{2} m l_1 l_2 (\cos \alpha \sin \beta - \sin \alpha \cos \beta) \ddot{\alpha}^2 \\ + \frac{1}{2} m l_1 l_2 (\sin \alpha \sin \beta + \cos \alpha \cos \beta) \ddot{\alpha} + \frac{1}{2} m g l_2 \sin \beta = 0 \end{cases} \quad (\text{A4})$$

For the double-pendulum model in Fig. 2, we choose the same two parameters as in the rigid rod to characterize the motions of the two masses. Following the same method, the motion equations of the two mass are

$$\begin{cases} (m_1 + m_2) l_1'^2 \ddot{\alpha} + (m_1 + m_2) l_1' \cos \alpha \ddot{x}_0 \\ + m_2 l_1' l_2' (\sin \alpha \cos \beta - \cos \alpha \sin \beta) \ddot{\beta}^2 \\ + m_2 l_1' l_2' (\sin \alpha \sin \beta + \cos \alpha \cos \beta) \ddot{\beta} + (m_1 + m_2) g l_1' \sin \alpha = 0 \\ m_2 l_2'^2 \ddot{\beta} + m_2 l_2' \cos \beta \ddot{x}_0 + m_2 l_1' l_2' (\cos \alpha \sin \beta - \sin \alpha \cos \beta) \ddot{\alpha}^2 \\ + m_2 l_1' l_2' (\sin \alpha \sin \beta + \cos \alpha \cos \beta) \ddot{\alpha} + m_2 g l_2' \sin \beta = 0 \end{cases} \quad (\text{A5})$$

Compared with the motion equations of the two models, it can be found that when the parameters of the double-pendulum model are scaled as $l_1' = l_1$, $l_2' = 2l_2/3$, and $m_1 = m_2/3$, the motion of the rigid rod can be derived from the double-pendulum model.

References

- [1] Abdel-Rahman, E. M., Nayfeh, A. H., and Masoud, Z. N., 2003, "Dynamics and Control of Cranes: A Review," *J. Vib. Control*, **9**(7), pp. 863–908.
- [2] Smith, O. J. M., 1957, "Posicast Control of Damped Oscillatory Systems," *Proc. IRE*, **45**(9), pp. 1249–1255.
- [3] Vaughan, J., Kim, D., and Singhose, W., 2010, "Control of Tower Cranes With Double-Pendulum Payload Dynamics," *IEEE Trans. Control Syst. Technol.*, **18**(6), pp. 1345–1358.
- [4] Singer, N. C., and Seering, W. P., 1990, "Preshaping Command Inputs to Reduce System Vibration," *ASME J. Dyn. Syst. Meas. Control*, **112**(1), pp. 76–82.
- [5] Algarni, A. Z., Moustafa, K. A. F., and Nizami, S., 1995, "Optimal Control of Overhead Cranes," *Control Eng. Pract.*, **3**(9), pp. 1277–1284.
- [6] Auernig, J. W., and Troger, H., 1987, "Time Optimal-Control of Overhead Cranes With Hoisting of the Load," *Automatica*, **23**(4), pp. 437–447.
- [7] Kim, D., and Singhose, W., 2010, "Performance Studies of Human Operators Driving Double-Pendulum Bridge Cranes," *Control Eng. Pract.*, **18**(6), pp. 567–576.
- [8] Kuo, T.-Y. T., and Kang, S. C. J., 2014, "Control of Fast Crane Operation," *Autom. Constr.*, **42**, pp. 25–35.
- [9] Manning, R., Clement, J., Kim, D., and Singhose, W., 2010, "Dynamics and Control of Bridge Cranes Transporting Distributed-Mass Payloads," *ASME J. Dyn. Syst. Meas. Control*, **132**(1), p. 014505.
- [10] Masoud, Z. N., Nayfeh, A. H., and Nayfeh, N. A., 2005, "Sway Reduction on Quay-Side Container Cranes Using Delayed Feedback Controller: Simulations and Experiments," *J. Vib. Control*, **11**(8), pp. 1103–1122.
- [11] Sun, N., Fang, Y., and Zhang, X., 2013, "Energy Coupling Output Feedback Control of 4-DOF Underactuated Cranes With Saturated Inputs," *Automatica*, **49**(5), pp. 1318–1325.
- [12] Balas, M. J., 1978, "Active Control of Flexible Systems," *J. Optim. Theory Appl.*, **25**(3), pp. 415–436.
- [13] Celentano, L., 2016, "Modeling of Flexible Robots With Varying Cross Section and Large Link Deformations," *ASME J. Dyn. Syst. Meas. Control*, **138**(2), p. 021010.
- [14] Flotow, A. H., 1986, "Disturbance Propagation in Structural Networks," *J. Sound. Vib.*, **106**(3), pp. 433–450.
- [15] Flotow, A. H., 1986, "Traveling Wave Control for Large Spacecraft Structures," *J. Guid. Control Dyn.*, **9**(4), pp. 462–468.
- [16] Saigo, M., Tanaka, N., and Tani, K., 1998, "An Approach to Vibration Control of Multiple-Pendulum System by Wave Absorption," *ASME J. Vib. Acoust.*, **120**(2), pp. 524–533.
- [17] O'Connor, W. J., 2003, "A Gantry Crane Problem Solved," *ASME J. Dyn. Syst. Meas. Control*, **125**(4), pp. 569–576.
- [18] O'Connor, W., and Habibi, H., 2013, "Gantry Crane Control of a Double-Pendulum, Distributed-Mass Load, Using Mechanical Wave Concepts," *Mech. Sci.*, **4**(2), pp. 251–261.
- [19] O'Connor, W. J., 2007, "Wave-Based Analysis and Control of Lump-Modeled Flexible Robots," *IEEE Trans. Robot.*, **23**(2), pp. 342–352.
- [20] Yang, T., and O'Connor, W., 2006, "Wave Based Robust Control of a Crane System," *IEEE/RSJ International Conference on Intelligent Robots and Systems (IROS)*, Beijing, China, Oct. 9–15, pp. 2724–2729.